

Blade Mistuning Analysis for Boundary Layer Inlet Flow Distortion-Tolerant Fan Blades

James B. Min, Milind A. Bakhle, Kirsten P. Duffy[†]

NASA Glenn Research Center, Cleveland, Ohio

[†]University of Toledo, Toledo, Ohio

NASA Glenn Research Center has tested the BLI2DTF propulsor including the fan rotor. BLI2DTF stands for Boundary Layer Ingesting Inlet/Distortion-Tolerant Fan. A comparison of the vibratory response between analysis results and experimental wind tunnel test results yielded reasonable agreement, yet some differences were noted. Blade mistuning effects have been identified as a potential cause for these differences. A tuned forced response analysis in a turbomachinery engine rotor system assumes that all of the blades are identical, so that the natural frequencies of individual blades are the same. In contrast to this assumption, the wind tunnel tests of the BLI2DTF rotor system revealed that the individual blade response frequencies varied. These variations in individual blade frequencies may be attributed to blade mistuning due to potential differences in the structural and material properties of individual blades. For an understanding of these variations, it is necessary to analyze the influence of blade mistuning on the BLI2DTF rotor system, which will provide a more precise assessment of its vibratory stresses and high cycle fatigue life. The purpose of the study was to investigate the influence of blade mistuning on the dynamic characteristics of this rotor system. At the same fan operation condition, a comparative forced response analysis was performed for both tuned and mistuned BLI2DTF rotor systems. A comparison of the results from these analyses found that the mistuning effects on the present BLI2DTF rotor system are notable. As a result, fan blade mistuning is to be considered a contributor to the levels of vibratory dynamic stresses observed during the wind tunnel experiment.

1. Introduction

Relocating the aircraft engines from a podded position on the wing or fuselage and embedding them into the airframe can improve vehicle fuel burn, weight, noise, and emissions through engine cycle improvement. The Blended-Wing-Body (BWB) architecture is particularly suitable for embedded engines, where aft placement on the airframe offers maximum BLI benefits. A main feature of the aircraft incorporating BLI propulsion is the embedded aft-mounted engines that ingest part of the fuselage boundary layer airflow [1-3]. The NASA Glenn Research Center (GRC) has been working on a first-of-its-kind boundary layer ingestion (BLI) inlet flow distortion-tolerant fan (DTF) rotor system (designated as BLI2DTF) to advance this concept. A detailed overview of this research as well as the wind tunnel test results are presented in Ref. [4].

The current authors previously published the findings of the force response analysis performed on the BLI2DTF rotor system [5, 6] as well as the experimental wind tunnel test results [7, 8]. Modeling results at design speed were used to assess the forced responses to those observed during wind tunnel testing. While a comparison of numerical analysis and experimental wind tunnel strain measurements indicated reasonable agreement, some differences in response values were observed. Dynamic strains were measured using strain gauges at four surface locations (Fig. 1b) on eight blades (Fig. 1c) as shown in Fig. 1. Strain gauges were installed in regions where high

dynamic strain was predicted for the structural modes and engine orders of interest, as illustrated by the contour plot (Fig. 1a). All gauges were placed on the pressure side of the blade to reduce their impact on fan performance. More details on strain measurement and measurement techniques are found in References 7 and 8.

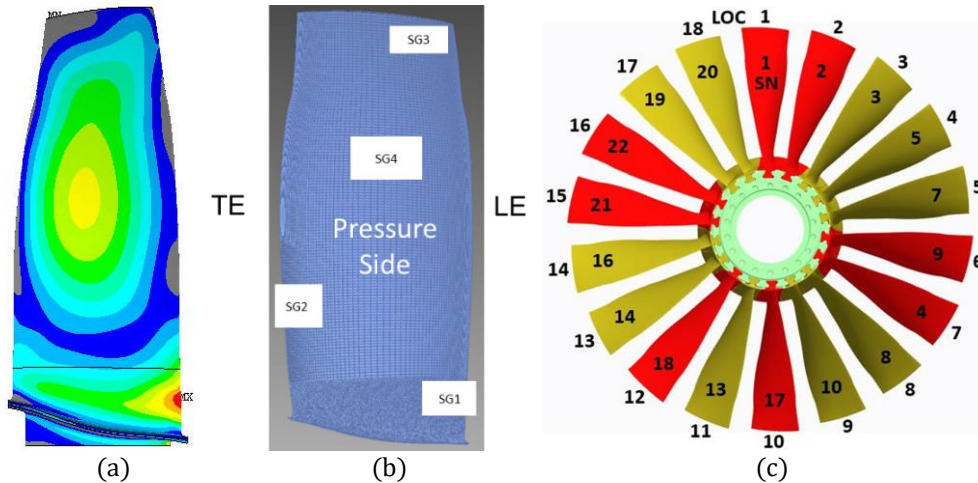


Figure 1. Optimal strain gauge locations determined from the modal strain on the BLI2DTF finite element mesh with gauged blade numbers shown in red color [5,7,8]

In the forced vibration response analysis of a turbomachinery bladed rotor system, cyclic symmetry is utilized, whereby all the blades are assumed to be identical. In reality, there are small differences in the structural properties of individual blades, possibly caused by manufacturing and material variations or in-service degradation, referred to as blade mistuning. The presence of mistuning breaks the nature of the cyclic symmetry configuration of the rotor system. As a result, the practical inability to completely eliminate blade mistuning can lead to a large increase in blade vibratory stresses, which can cause elevated levels of high cycle fatigue (HCF) life problems that ultimately lead to engine failures, posing a significant safety and cost concern. Previous study has also shown that the presence of high vibration energy in a few blades can result in response amplification of 100 percent or more in some blades [9, 21, 22]. This concern necessitated further research into the mistuning effects that may have influenced the fan blade response data during the BLI2DTF wind tunnel test. All of the blades were assumed to be same in our earlier research [5, 6], i.e., the analysis was based on the assumption of a tuned blade row in which the individual blades are identical, are identically mounted and evenly spaced on the disk, and their natural frequencies and mode shapes are identical. On the other hand, certain blades in a mistuned system are likely to have considerably higher forced vibration responses than the idealized tuned system.

Mistuning research has led to significant developments in computational modeling and analytic approaches in recent years. There has been an emphasis on the development of reduced order models (ROM), which enable the analysis of high fidelity mistuning models with a large number of degrees of freedom in realistic computer times. Rather than finite element modeling and analysis of the entire 360-degree fan rotor geometry, various reduced-order modeling techniques that efficiently analyze the structural mistuning responses of a bladed disk have been developed. Component mode synthesis or related methods [10-16], as well as classical modal analysis with a mistuning projection [17], are examples of these techniques. For many methods developed to date,

reduced-order modeling techniques have been developed by substructuring a bladed disk into disk and blade components [10, 11]. Castanier et al. [12-15] established a mistuning analytical modeling technique in a component-based reduced-order model using a mistuning projection method that projects stiffness mistuning matrices in physical coordinates to the normal modes of a tuned cantilevered blade fixed at the disk-blade interface. Few studies have also looked at the combined effect of aerodynamic coupling and mistuning on the forced response, which is accomplished by adding aerodynamic effects into structural mistuning [9, 16, 18, 19]. Significant progress has been made in the development of methodologies for ROM mistuning analysis. The current study uses the component mode synthesis (CMS)-based component mode mistuning (CMM) method [15, 18] in conjunction with the Ansys® code for small stiffness mistuning dealing with slight variations in the Young’s modulus of the blades. Given that the blade shape is not drastically altered, this methodology was determined to be well suited to the simulation of BLI2DTF. The displacements at the blade root are assumed to be very small in comparison to those at the airfoil portion of each blade for the current BLI2DTF fan design configuration; thus, the contribution of this feature to the mistuning projection of the boundary modes defined at the blade-disk boundary [13] is not considered in the current analysis modeling. A major advantage of this method is that arbitrary patterns of mistuning in the physical stiffness matrices can be efficiently and accurately implemented in a compact reduced-order model using modal mistuning values. If only stiffness mistuning is assumed, an equivalent stiffness mistuning parameter can be computed as described in Section 4.

The blade tip timing laser probe data gathered during wind tunnel tests on a BLI2DTF rotor system exhibited variations in the amplitude and frequency of the blade response [7]. This data suggests that the observed variation in blade-to-blade response is caused in part by mistuning effects. Previous research has also shown that structural and aerodynamic interactions can play a role in the mistuned response problem [9, 16, 18, 19]. The present study, on the other hand, did not aim to examine mistuning concerns by coupling aerodynamic motion-dependent aero-damping terms and structures for aerodynamic and structural mistuning interactions. The only aerodynamic terms employed in the present study are the forcing functions as an aerodynamic input that are relevant to the wind tunnel test.

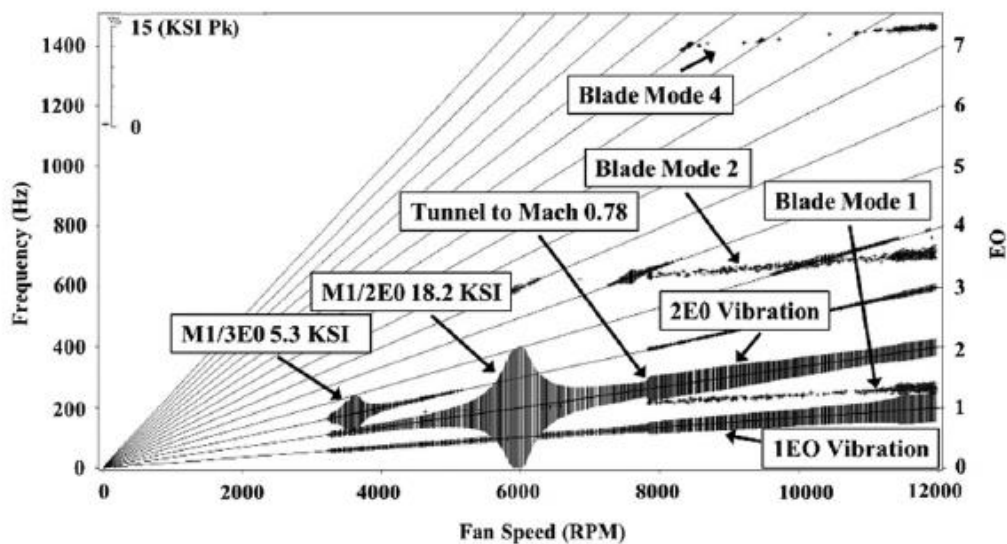


Figure 2. 2nd Engine Order in Mode 1 (M1/2EO) condition exhibited in BLI2DTF blade vibration Campbell diagram during wind tunnel test rig startup at blade root [8]

The goal of the present study was to look at the effects of mistuning on the BLI2DTF rotor system, utilizing frequency measurement data from a wind tunnel test to compute the effects of fan blade mistuning on the forced responses with BLI flow distortion. A more specific purpose was to investigate the significance of mistuning using the particular case of the BLI2DTF rotor's 2nd Engine Order in Mode 1 (2EO M1) critical condition (namely, a possible crossing at 51 percent off-design speed), which can be encountered near an engine order resonance (Fig. 2). The current study assumes that blade-to-blade variations can be completely defined by maximum response frequency recorded during the BLI2DTF experimental wind tunnel tests. In the future, the blade mistuning frequencies will be measured with a rap test as a more direct method.

2. Structural Modeling and Forced Response Analysis Approaches

Individual blade modeling based on the assumption of a single cantilevered beam mounted at the blade root has limitations for accurately assessing the dynamic behavior of a full-bladed rotor system with the possibility of local mistuning. The forced response analysis for a case of 2EO in Mode 1, as represented in the Campbell diagram of the BLI2DTF rotor system (Fig. 3) was performed for the current study.

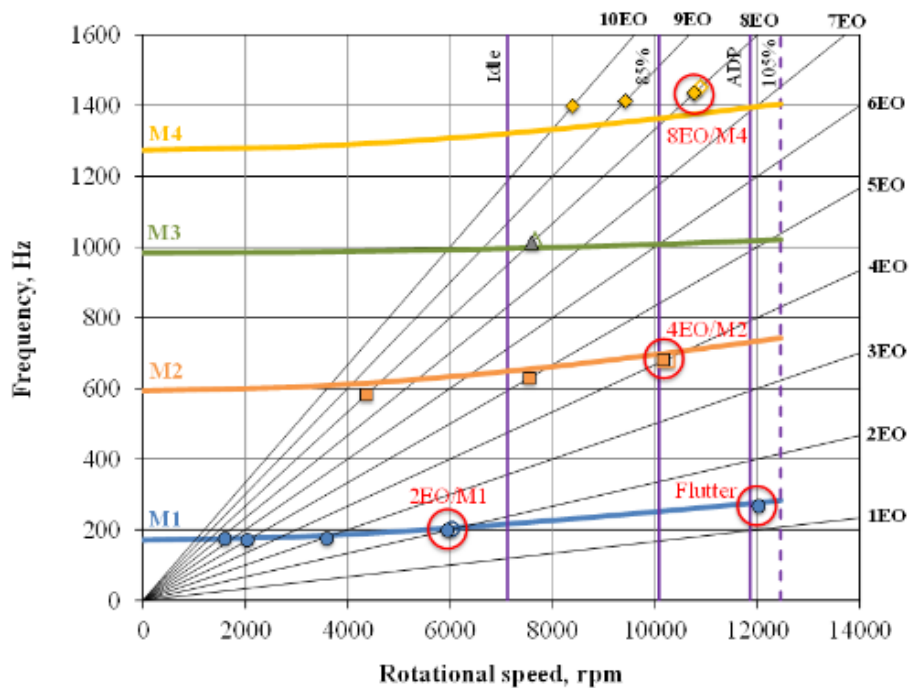


Figure 3. Campbell diagram for the BLI2DTF created using the model and experimental test data (solid lines — FEA; filled symbols — wind tunnel results; unfilled symbols vacuum spin rig results; vertical lines — rotor speed lines; diagonal lines — engine order (EO) excitation frequencies)

The BLI2DTF fan is a 22-inch diameter bladed disk with eighteen titanium blades [8]. The cyclic symmetry finite element forced response modeling approach was used in the present study, both ‘with mistuning’ and ‘without mistuning (tuned)’ to examine the mistuning effects on the

blade vibratory stress amplitudes. The individual blade modal data were computed using the same cyclic symmetric finite element model displayed in Fig. 4 to examine the mistuned bladed disk rotor system. More details on structural modeling techniques are found in Ref. 5. The finite element structural model was developed as part of the BLI2DTF fan rotor design process. For the airfoil region, the sector geometry of the fan rotor was meshed with higher-order 20-node hexahedral elements. The airfoil platform and disk portion were densely meshed with higher-order 10-node tetrahedral elements for more accurate stress prediction in local high stress regions. A symmetric sector was created to place eighteen blades symmetrically around the disk, resulting in a 20-degree sector. To effectively capture the bending stiffness, the airfoil was meshed with four hexahedral elements through the thickness. Fig. 4 depicts the complete mesh of a sector geometry with 557,554 elements and 992,548 nodes. The CMM mode projection approach [15] was then used to generate the modal participation data of cantilevered-blade normal modes in tuned system normal modes from the tuned finite element model into the modal coordinates and the effect of mistuning was added.

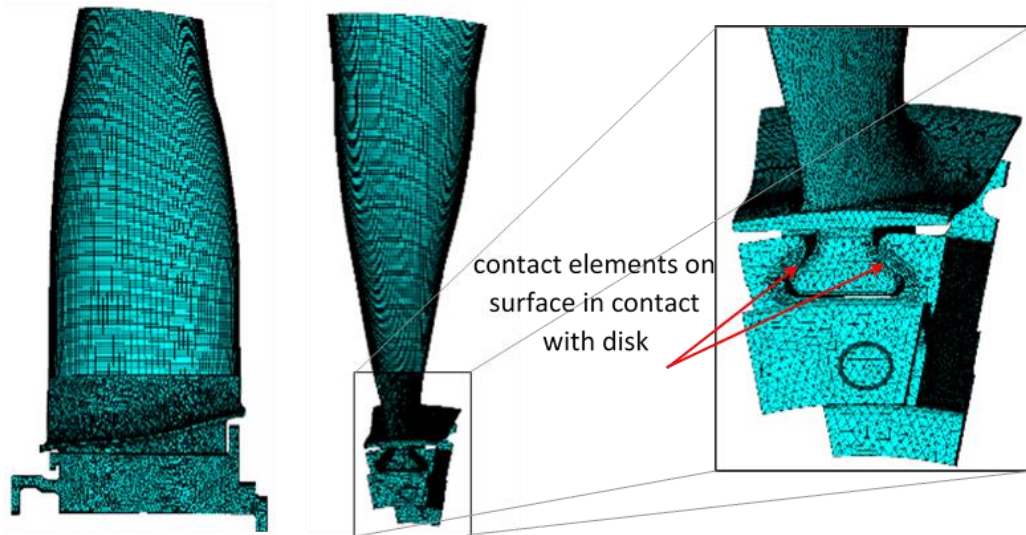


Figure 4. Finite element mesh of a cyclically symmetric base sector of BLI2DTF

The modes and natural frequencies of the mistuned bladed disk are determined by the solution of this modal analysis. The mode superposition method is then used to carry out the forced response [20]. This analysis result provides the details of the effect of mistuning on the 2EO in Mode 1 with mistuning.

3. Aerodynamic Modeling and Analysis Approaches

The BLI2DTF fan was also subjected to an aerodynamic study in order to compute the steady and unsteady pressures on the blades that would be employed in the finite element forced response analysis model. To compute the vibratory dynamic stresses, the unsteady harmonic pressure was modeled as blade excitation force. While the 2EO unsteady excitation at the off-design speed (51 percent of the design speed) was required for the subject analysis, due to the unavailability of aerodynamic distortion pressure information at this off-design speed, the 1EO aerodynamic distortion pressure obtained at the design speed was used for the present analysis. The reasoning

behind this substitution was that the 1EO aerodynamic forcing is comparable to the 2EO forcing in prediction as shown in Fig. 5, and applying it consistently allows for the desired direct comparison of tuned and mistuned analyses.

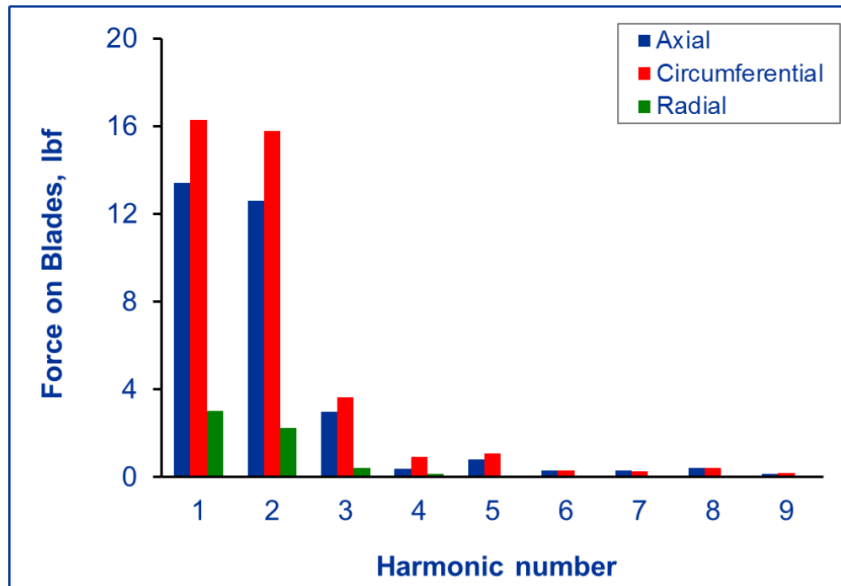


Figure 5: Blade unsteady force in terms of EO's (harmonic numbers) at design speed [5]

A brief overview of the previously reported aerodynamic analysis at design speed (Figs. 6 and 7) [6] is provided as follows: Only the fan rotor is included in the current aerodynamic model. The boundary layer ingesting (BLI) inlet is not included in the aerodynamic computations. Instead, the boundary layer flow distortion extracted from a separate flow analysis was prescribed as an inflow boundary condition upstream of the rotor. It is expected that the first-order effects of the strong BLI distortion are captured adequately.

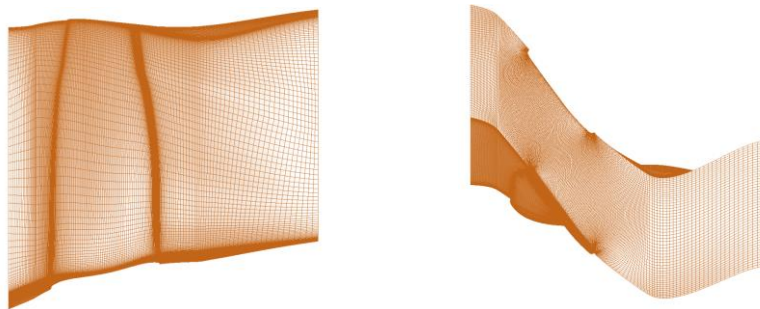


Figure 6. Aerodynamic mesh azimuthal and radial views for one blade passage [6]

In this part of the work, a fan rotor flow solution is initially obtained using the circumferential average of the BLI distortion. Following this analysis, the BLI distortion inflow profile, which contains flow quantities that vary in both the circumferential and radial directions, was used as the inflow boundary condition. For the distortion patterns of the 1 EO aerodynamic condition at design speed, the relevant flow quantities required to properly prescribe the inlet boundary condition are illustrated in Fig. 7.

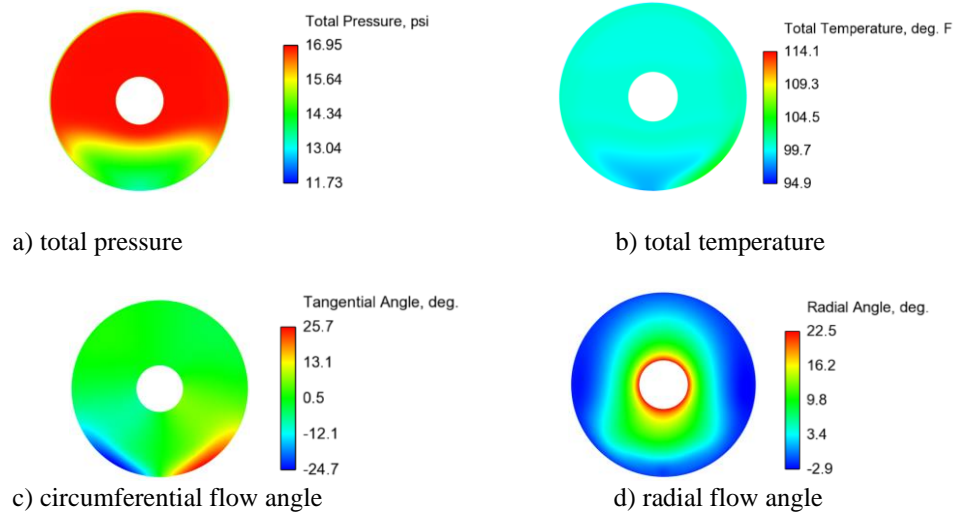


Figure 7. Distributions of flow profiles at the inflow plane for BLI distortion analyses for the BLI2DTF design condition [6]

As already stated, while the 2EO crossing at the off-design speed (51 percent of the design speed) was the case for the subject mistuning analysis, the 1EO aerodynamic pressure values obtained at the design speed were used in a 2EO pattern for the current mistuning analysis. The time-averaged aerodynamic pressure on the blade surfaces was computed. Fig. 8 depicts its distribution on each side of the blade surfaces. This steady-state pressure load was applied to the finite element blade structural model prior to the cyclic symmetry modal analysis to compute a pre-stressed state condition at design speed.

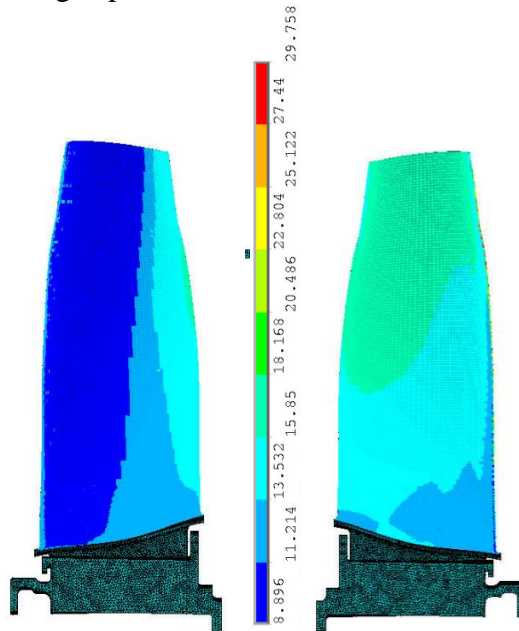


Figure 8. 1EO steady-state aerodynamic pressure (psi) distribution contours on blade pressure surfaces (left) and suction surfaces (right) mapped on a finite element cyclic symmetry sector model

For the tuned model, the free vibrations of the cyclic symmetric BLI2DTF rotor system have the characteristic that the mode shapes vary sinusoidally in the circumferential direction. This is indicated in Fig. 9 by nodal lines across the disk known as nodal diameters (ND), which are defined as the number of diameters in the rotor along which the displacements are zero.

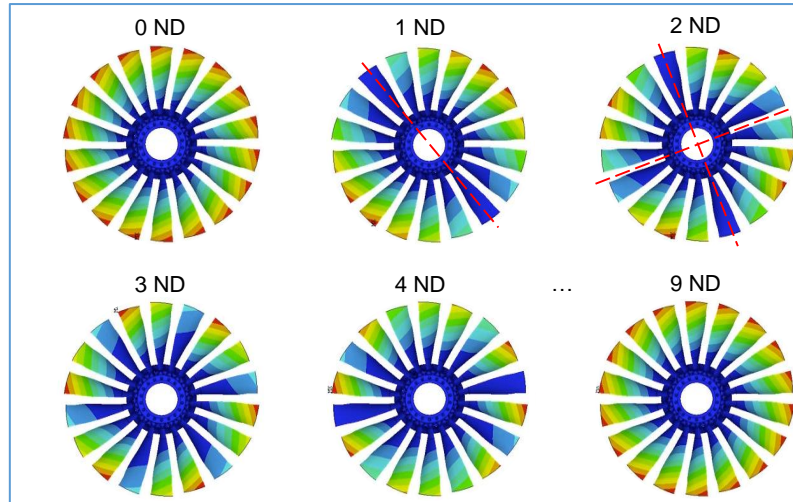


Figure 9. BLI2DTF fan nodal diameter (ND) patterns for mode 1, with the largest deformation shown in the red color contour. The dashed lines line represents zero displacement.

The natural frequencies calculated by the pre-stressed finite element modal analysis of the BLI2DTF rotor are plotted in terms of nodal diameters in Fig. 10. In this figure, the nearly horizontal curves represent assembled fan rotor modes dominated by blade motions, whereas the slanted curves represent assembled fan rotor modes interacting with disk motions. The rapid

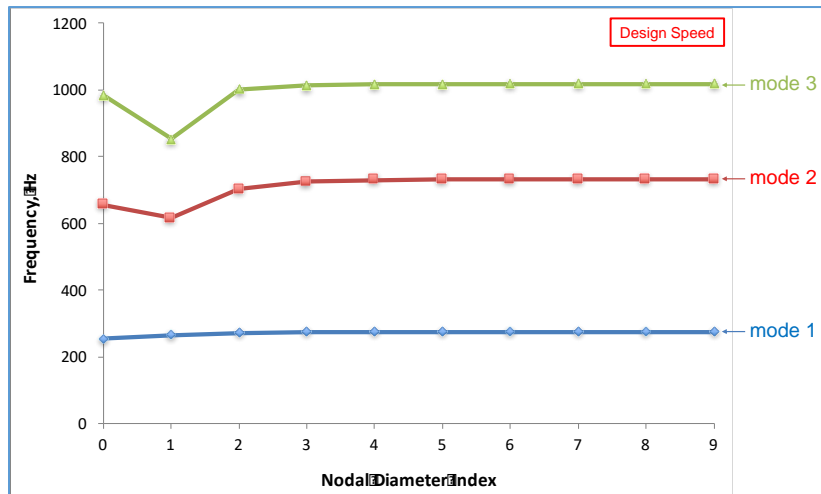


Figure 10. The natural frequency map of tuned BLI2DTF in terms of nodal diameters for the first three modes for the design speed condition

change in frequency of disk-dominated modes at one nodal diameter (1 ND) is attributed to the disk-induced blade-disk interactions. The structural connection through the disk is often the main energy transfer path from blade to blade, which is related to the interaction of disk and blade dynamics. The variation of natural frequencies with nodal diameter (Fig. 10) shows that the first three mode families are well-separated and there is some limited blade-disk interaction for modes 2 and 3. When analyzing with a finite element model, the elastic deformation resulting from disk motion is incorporated into the blade motion, and so the stress state for a blade in a bladed disk assembly can differ from that of a cantilevered blade. Earlier research [12, 15, 21, 22] has demonstrated that considerable increases in the mistuned forced response (100 percent or more in some blades), relative to the tuned response, are likely to occur in veering regions where two or more modes have close eigenfrequencies. However, the current BLI2DTF bladed disk in Fig. 10 does not exhibit any typical veering characteristics as there are no closely spaced modes or significant modal interactions.

Knowing that the modes of the BLI2DTF blade are well separated from one another, suggesting no dependency, mode interactions are not required in the current resonant forced response study with mistuning. Unless the modes are closely spaced, the fan blade forced response near a crossing (resonance) is dominated by a single nodal diameter mode. As a result, it was assumed for this analysis that 2EO excitation caused by a particular unsteady pressure force distribution corresponds to each blade passing through two evenly spaced forcing peaks in each rotation. This type of forcing only excites modes that match the engine order, so the 2ND mode would be excited by the 2EO unsteady excitation pressure force. As seen in the Campbell diagram (Fig. 3), the 2EO forcing excites the natural frequency of the 2 ND pattern of Mode 1, which has a 1.98 percent average damping ratio measured from wind tunnel testing.

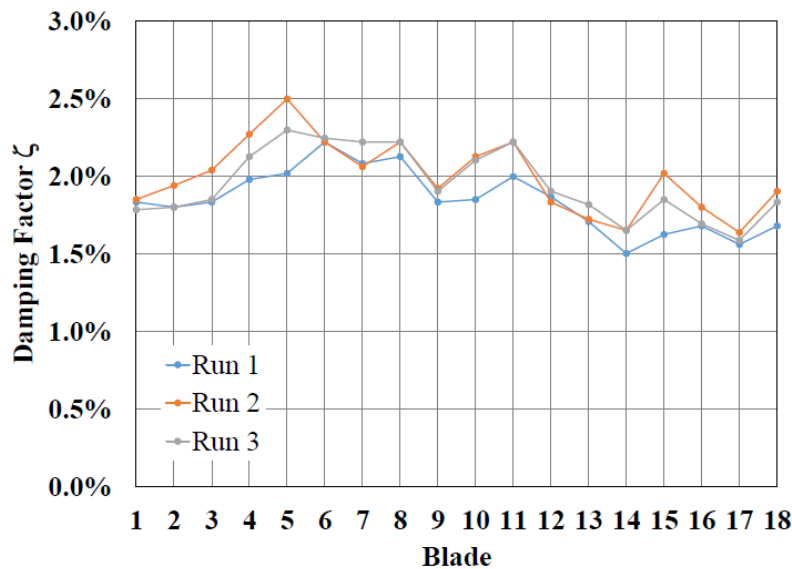


Fig. 11 Blade damping factor for three sweeps of 2EO Mode 1 in the wind tunnel

The NASA Glenn Research Center Dynamic Spin Facility (spin rig) [7] was also used to test two of the eighteen blades in vacuum before the wind tunnel test to determine the blade damping factors and resonance frequencies in the absence of aerodynamic damping. Based on the four-probe non-contacting stress measurement system (NSMS), the two blades in the vacuum spin rig had very

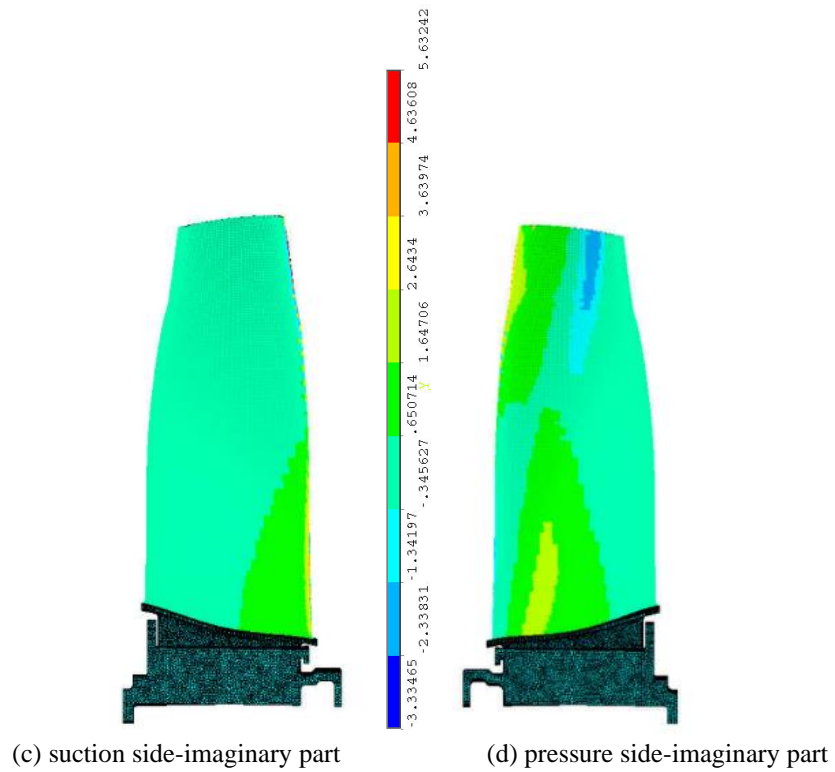
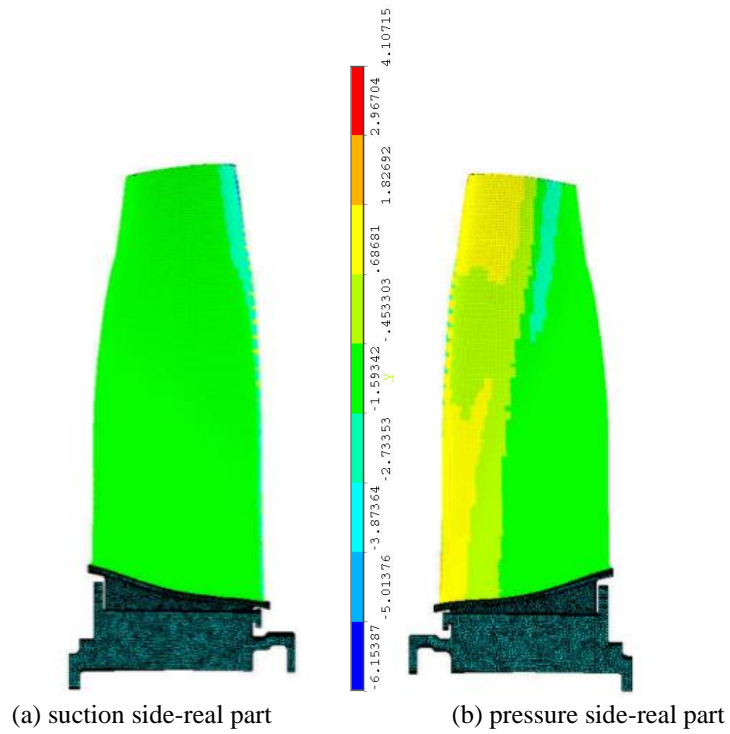


Figure 12. Unsteady real and imaginary aerodynamic pressure (psi) distribution on blade suction surfaces (a, c) and pressure surfaces (b, d) at design speed for 1EO conditions

low damping levels, roughly 0.19 percent with 2EO Mode 1. The spin rig damping is substantially lower than the wind tunnel result. Clearly, the airflow over the blades adds significant aerodynamic damping in this resonance mode of the blade. Figure 11 shows the damping factors for each blade in the wind tunnel test in three separate runs. The similarity of the pattern indicates that there has been no alteration in the qualities of the blades (such as blade damage) between runs. The present analysis applied the 1.98 percent average damping ratio measured from wind tunnel tests in Fig. 11 for all blades, even though the damping ratios for each individual blade indicate substantial variability [7, 23].

While the effects of structural and aerodynamic coupling with mistuning are not directly formulated within the equation of motion, steady and unsteady aerodynamic pressure values from an external aerodynamic code [6] are mapped onto finite element meshes for forced response analysis with mistuning. The pressure quantity displayed in Figs. 8 and 12 represents the 2EO steady and unsteady surface pressure applied to the finite element cyclic symmetry forced response analysis model with and without mistuning.

4. Mistuning Modeling and Analysis Approaches

In order to develop a CMM-based reduced-order model for mistuning analysis, two tuned finite element models are required: a sector model consisting of an airfoil-part and disk-part (illustrated in Fig. 4) and an airfoil-alone model are required. The normal modes of the tuned fan rotor system are obtained using cyclic symmetry pre-stressed finite element modal analysis, as previously stated in Section 2. The blade-alone modal analysis yields the cantilevered-blade normal modes. In addition, the CMM-based mistuning analysis model must incorporate the degrees of freedom (DOF) at the interface between the blade and the disk. As stated in Section 1, the current study was carried out by integrating the proportional small stiffness mistuning methodology. If there is a large mistuning, such as fractures at the tip of a blade or a significant geometric deviation, the model needs to incorporate many more tuned-system modes or tuned components (disk and blade) modes. This is because the mass or stiffness matrices can be substantially changed, and the modes of a mistuned blade can be very different from those of a tuned blade. The present analysis did not account for such a large amount of mistuning since it was not expected to be present in the BLI2DTF fan rotor.

For a small proportional mistuning condition, the mistuning is introduced to the full finite element model by varying Young's modulus in the blade elements [15]:

$$E_n = (1 + \delta_n)E_o, \quad n = 1, 2, 3, \dots, N \quad (1)$$

where n is the blade number, δ_n is the mistuning value for blade n , and N is the total number of blades. A mistuned Young's modulus value is described for each individual blade. It was assumed that, as the result, the percentage deviations of the cantilevered blade natural frequencies are the same for all modes, and the mode shapes of the tuned and mistuned blades are the same. When this occurs, the natural frequencies of the blade are altered by a common factor. A frequency-dependent mistuning parameter is calculated in order to individually change each natural or resonant frequency:

$$\delta_n = \delta f_i^n = (\bar{\omega}_i^n / \omega_i^n)^2 - 1 \quad (2)$$

where ω_i^n is the i^{th} tuned natural frequency of blade n and $\bar{\omega}_i^n$ is the i^{th} measured natural or resonant frequency of blade n .

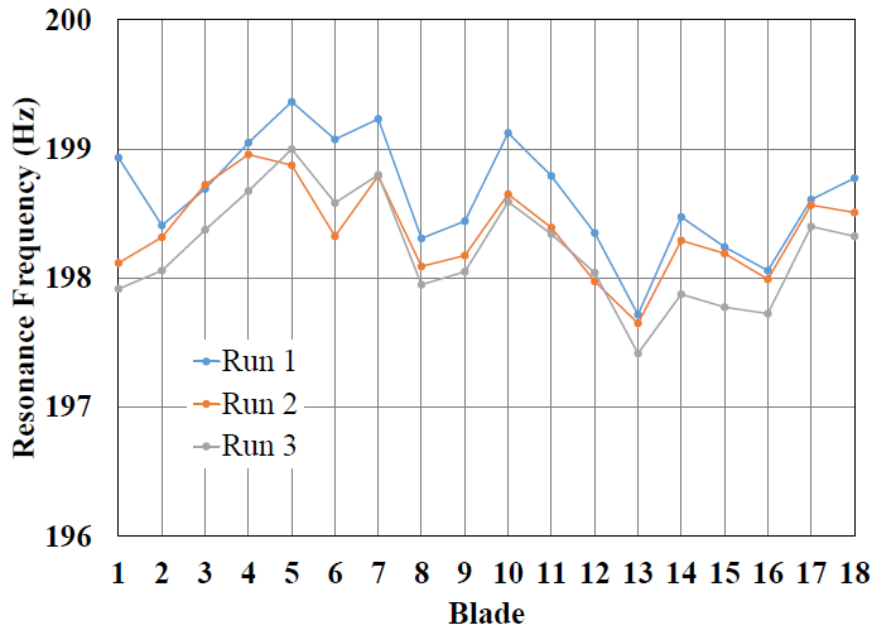


Figure 13. Variations in resonant frequency detected in wind tunnel testing for individual blades at the critical 51 percent off-design speed for 2EO, Mode 1 condition. The 2ND frequency from the tuned analysis model is 201 Hz.

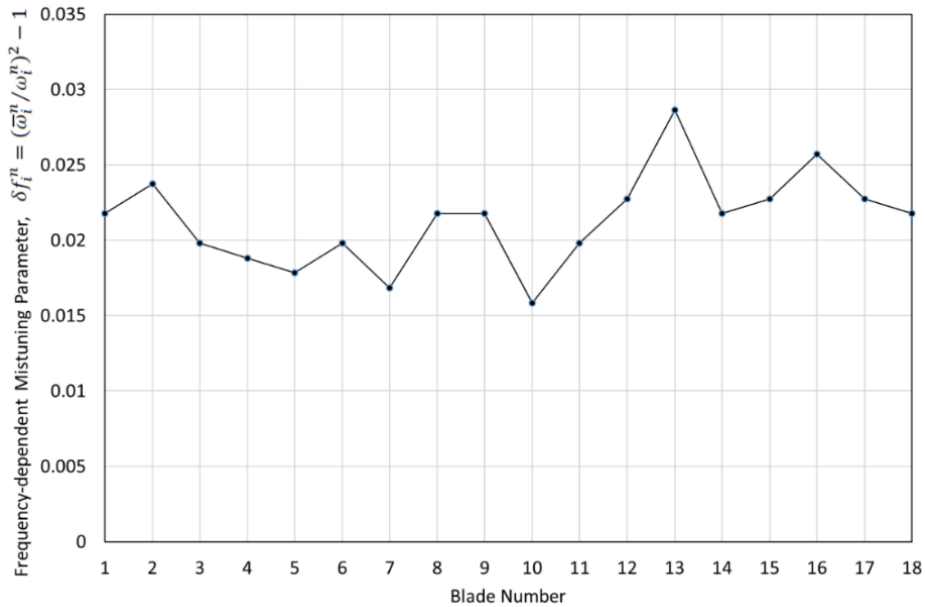


Figure 14. Mistuning parameter variations in blades and mistuning patterns utilized for the condition of 2EO, Mode 1; ω is the tuned natural frequency, and $\bar{\omega}$ is the measured resonant frequency of bladed disk system

Fig. 13 displays the BLI2DTF blade frequency variations measured for individual blades during wind tunnel tests and refers to the frequency predicted by the tuned analytical model. The component mode mistuning model for the present investigation makes use of these bladed disk system frequencies. It should be noted that the mistuning of a specific mode of 2EO in Mode 1 was only considered in this investigation. The mistuning parameters, δf_i^n , considered in the analysis for each blade are presented in Fig. 14.

The equation of motion, Eq. (3), for a mistuned system for harmonically varying forced response is solved in Ansys[®] code as follows:

$$([K^s] - \Omega^2[M^s])\{u^s\} = \{F^s\} \quad (3)$$

where

- $[K^s]$ = stiffness matrix of the bladed disk rotor system
- $[M^s]$ = mass stiffness of the bladed disk rotor system
- $\{F^s\}$ = complex load vector (unsteady aerodynamic pressure)
- $\{u^s\}$ = displacement vector
- Ω = engine order (EO) forcing frequency
- s = represents that matrices refer to the entire 360-degree system.

Eq. (3) is transformed into modal space by

$$\{u^s\} = [\Phi^s]\{q^s\} \quad (4)$$

where

- $[\Phi^s]$ = eigenvectors of the full system
- $\{q^s\}$ = modal coordinate vectors

As previously stated, stiffness mistuning can be defined as a variation of a system's nominal stiffness; thus, the stiffness matrix can be expressed as,

$$[K^s] = [K_o^s] + [K_\delta^s] \quad (5)$$

where subscript o indicates the nominal value and δ indicates deviation from the nominal value. If the mistuning is assumed to be in the blade only and to be proportional mistuning [15],

$$[K_\delta^s] = B_{diag}[\delta f_i^n [K_o^s]] \quad (6)$$

where

- $[K_o^s]$ = nominal stiffness matrix for a blade, including any pre-stress effects
- δf_i^n = dimensionless eigenvalue frequency mistuning deviation parameters for blade n , being considered as deviation in Young's modulus
- $B_{diag}[\cdot]$ = block diagonal matrix

This implies that Eq. (6) is suitable for implementing mistuning by individually modifying the material stiffness of each blade. Combining Eq. (4) through Eq. (6), the mode-superposition forced response equation, Eq. (7), is expressed and solved,

$$\left([A^s] + \sum_{n=1}^N \{ [\Phi_n^s]_{blade}^T \delta_n [K_o] [\Phi_n^s]_{blade} \} - \Omega^2 [I] \right) \{ \{q^s\} \} = [\Phi^s]^T \{F^s\} \quad (7)$$

where the matrix with a subscript “blade” represents the blade-only degrees of freedom from the system eigenvectors.

where

- $[A^s]$ = diagonal matrix of the rotor natural frequencies squared
- $[I]$ = identity matrix
- $[\Phi^s]^T$ = transpose of eigenvectors of the full system $[\Phi^s]$
- δ_n = mistuning value for blade n

The degrees of freedom of Eq. (7) is significantly smaller than that of Eq. (3) in the computational processes. Once again, it should be noted that both tuned and mistuned forced response evaluations were performed under identical load and structural damping conditions. To allow for a direct comparison of tuned and mistuned forced response simulations, a total damping of 1.98 percent as combined structural and aerodynamic damping was used in the current investigation. Typically, aerodynamic damping is a function of the nodal diameter pattern or interblade phase angle, but it was treated as a constant value in this analysis.

5. Results and Concluding Remarks

First, the objective of this work is to evaluate a forced response mistuning approach and analysis that may be used as a guide in the design of a robust distortion-tolerant fan (BLI2DTF) rotor system. Second, a specific case of the BLI2DTF rotor’s 2nd engine order unsteady pressure excitation acting on the fan blades in Mode 1 (2EO Mode 1) with and without mistuning has been investigated at a critical part-speed condition near an engine order crossing (resonance) indicated in Figs. 2 and 3, where the excitation forcing frequency range was limited to a small range around the 1st mode (Mode 1) frequency.

The tuned response shown in Figs. 15 and 16 is the same for all 18 blades. The resonance with mistuning occurs at various excitation frequencies for separate blades, as shown in Fig. 15, with the largest response amplitude occurring at 198.7 Hz on blade number 2 and the lowest response amplitude occurring on blade number 3 at 198.4 Hz. Furthermore, as indicated in Fig. 15, blade mistuning can substantially affect the forced response compared to the tuned response. It was also noticed during the current investigation that there is a frequency shift between the tuned CMM resonance frequency and mistuned CMM resonance frequencies, which is known as the cyclic modeling error [24] in the CMM modeling method and can be interpreted as deviations of the actual eigenvalues from the tuned ones. Thus, the averaged wind tunnel resonance frequency was utilized to update tuned CMM resonance frequency using the method outlined in Ref. 24. When small mistuning methods (such as CMM) are applied, the mistuning pattern usually has a zero

mean and thus the Young's modulus or bulk modulus of the tuned CMM model is aligned with the average modulus from the experiments [25].

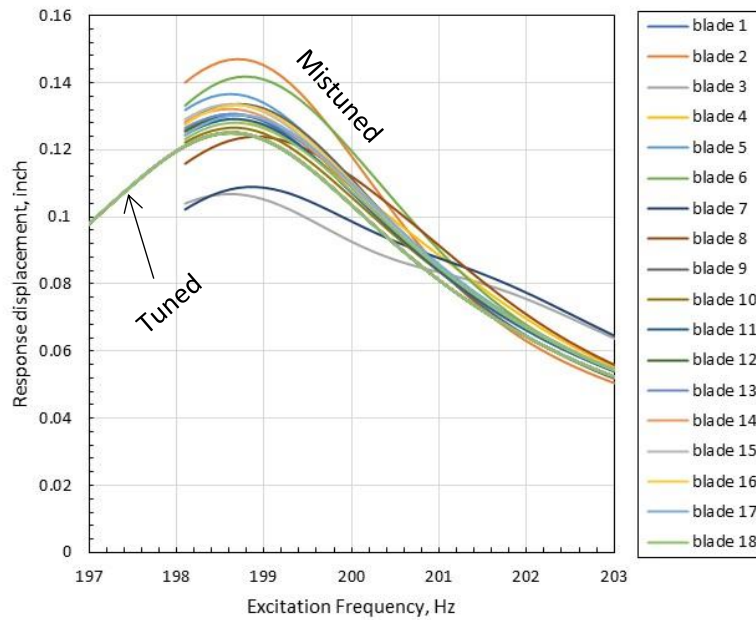


Figure 15. Comparison between tuned and mistuned displacement responses at SG locations

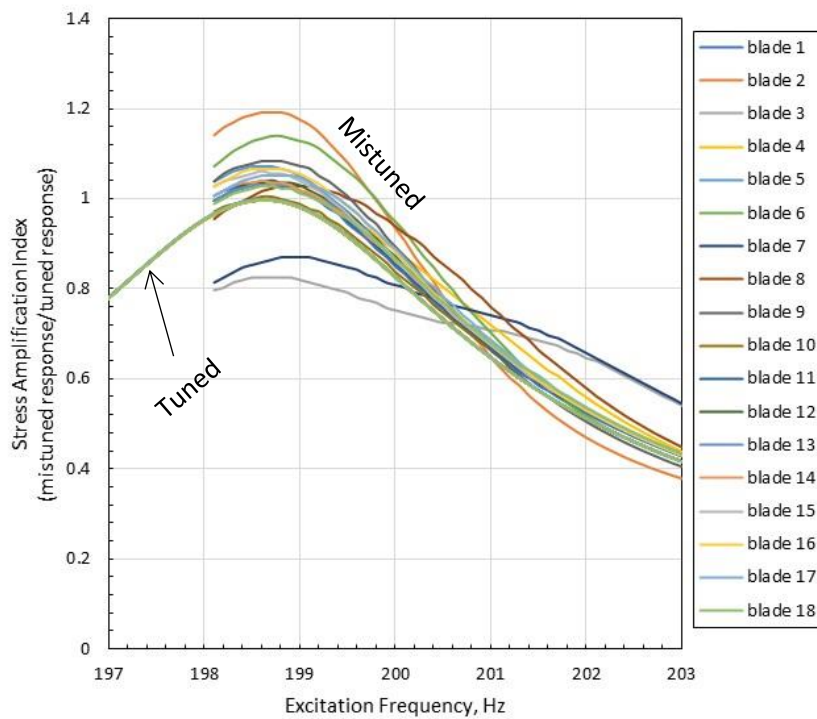


Figure 16. Comparison between tuned and mistuned stress amplification index at SG locations

The amplitude magnification factor is commonly used to quantify the degree of mistuning effects on the bladed disk forced response. The normalized forced response stress amplitudes, i.e., stress at a strain gauge location, on each of the eighteen blades of the BLI2DTF rotor system are shown in Fig. 16. It should be reiterated that the current analysis was performed using the 1EO unsteady pressure excitation at design speed because aerodynamic distortion pressure information at this off-design operating condition is unavailable. Thus, the measured blade amplitudes of the 2EO Mode 1 response for each blade were not directly compared with the current analysis results. The amplitude magnification indices were instead used to compare tuned and mistuned forced responses. The normalized stress amplification index (factor) was calculated by normalizing the mistuned forced response stresses at each frequency by a maximum tuned forced response stress at the resonance condition corresponding to the stress amplitude of interest in the current study. That is, the largest mistuned forced response amplitude is of our primary interest. The mistuned response amplification index larger than 1 indicates the increase in stresses due to mistuning. These amplification factors provide a quantifiable assessment when the effect of mistuning is critical during the BLI2DTF blade design process. As illustrated in Fig. 17, at its resonance frequency of 198.7 Hz, the maximum blade amplitude has increased by roughly 19% in blade number 2 when compared to a tuned blade.

The present study has used a comparative forced response calculation for both tuned and mistuned BLI2DTF rotor systems at the same fan operation condition to demonstrate the effect of blade mistuning. While the current analysis shows a stress amplitude increase of 2.2% to 19% as a result of mistuning for the potential resonance condition at 2EO in Mode 1, it can be significantly higher depending on other engine orders of excitations and modes. In terms of comparing analysis with wind tunnel measurements, the amplitude variations in the wind tunnel for 2EO in Mode 1 ranged between 8% and 19% from the average amplitude, depending on the test run [7], which is similar to the analysis results.

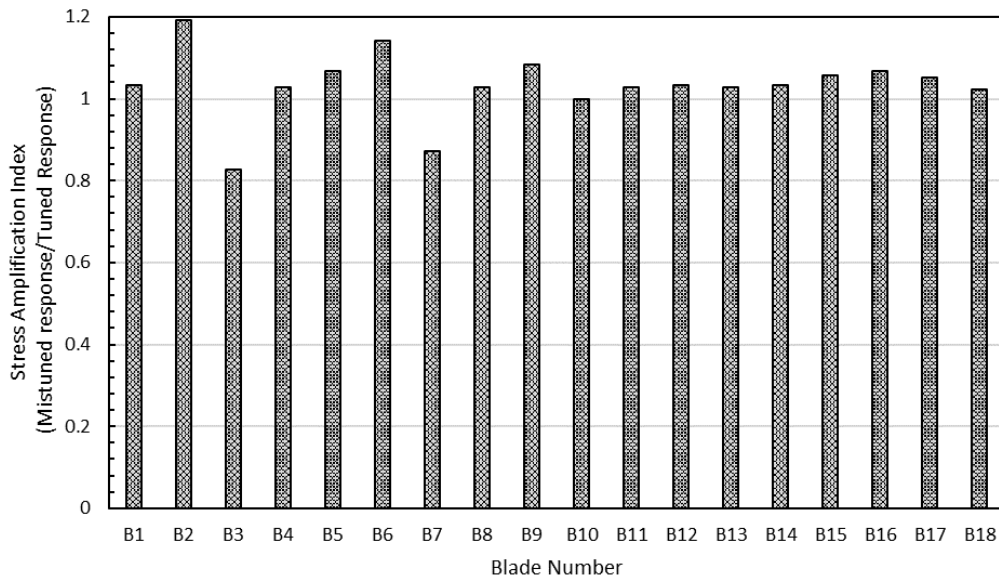


Figure 17. Stress amplification index at a resonance frequency of 198.7 Hz

Also, as shown in Figs. 15 and 16, analysis results indicate that resonance does not occur simultaneously in blades. When the bladed disk is operated, all of the mistuned blades on the rotor display their maximum response at different resonance frequencies.

Meanwhile, the present study has used a constant damping value averaged from the damping of each individual blade, but more validations are needed to address the following challenge: the effect of damping variances seen in individual blades during wind tunnel testing, in combination with stiffness mistuning, on the forced response of the BLI2DTF blade rotor system, which may affect the present analysis results. While mistuning is involved in the coupling of aerodynamic motion-dependent aerodynamic damping terms and structures for aerodynamic and structural mistuning interactions, such effects were not explored in the present analysis and will be addressed in the near future.

Although there are identified areas for further research and exploration, the current mistuning analysis results provide insight into complexity and uncertainty concerns, such as optimizing blade designs, adjusting manufacturing processes, or implementing control solutions, with advantages such as more informed confidence checks in tuned analysis predictions. Using data from the BLI2DTF wind tunnel test, a method for analyzing fan blade mistuning has been demonstrated.

Acknowledgments

Support of this work by NASA Advanced Air Transport Technology Project is greatly appreciated. The authors would also like to thank Prof. Robert Kielb of Duke University, Prof. Kiran D'Souza of Ohio State University, and David Arend of NASA Glenn Research Center for reviewing the paper.

References

1. Greitzer, E. M., et al., "N+3 Aircraft Concept Designs and Trade Studies, Final Report," NASA/CR—2010-216794/VOL1, NASA, 2010.
2. Liebeck, R., "Blended-Wing-Body Design of the Subsonic Transport," 40th AIAA Aerospace Sciences Meeting & Exhibit, AIAA-2002-0002, AIAA, January 2002.
3. Hardin, L. W., Tillman, T. G., Sharma, O. P., Berton, J. J., and Arend, D. J., "Aircraft System Study of Boundary Layer Ingesting Propulsion," AIAA Paper 2012-3993, July-August 2012.
4. Arend, D. J., Wolter, J. D., Hirt, S. M., Gazzaniga, J. A., Cousins, W. T., Hardin, L. W., Voytovych, D. M., Sharma, O. P., "Experimental Investigation of an Ultra-High Bypass Ratio Embedded Boundary Layer Ingesting Propulsor for Subsonic Cruise Aircraft", ASME Paper GT2020-15695, ASME Turbomachinery Technical Conference and Exposition (Virtual), September 21-25, 2020.
5. Min, J. B., Reddy, T. S. R., Bakhle, M.A., Coroneos, R. M., Stefko, G. L., Provenza, A. J., Duffy, K. P., "Cyclic Symmetry Finite Element Forced Response Analysis of a Distortion-Tolerant Fan with Boundary Layer Ingestion," AIAA Paper 2018-1890, AIAA Aerospace Sciences Meeting, January 8-12, 2018.
6. Bakhle, M. A., Reddy, T. S. R., Coroneos, R. M., Min, J. B., Provenza, A. J., Duffy, K. P., Stefko, G. L., Heinlein, G. S., "Aeromechanics Analysis of a Distortion-Tolerant Fan with Boundary Layer Ingestion," AIAA Paper 2018-1891, AIAA Aerospace Sciences Meeting, January 8-12, 2018.
7. Duffy, K. P., Provenza, A. J., Bakhle, M. A., Min, J. B., Abdul-Aziz, A., "Laser Displacement Measurements of Fan Blades in Resonance and Flutter During the Boundary Layer Ingesting Inlet and Distortion-Tolerant Fan Test," AIAA SciTech Forum, AIAA Paper 2018-1892, January 2018.

8. Provenza, A. J., Duffy, K. P., Bakhle, M. A., “Aeromechanical Response of a Distortion-Tolerant Boundary Layer Ingesting Fan,” ASME Paper GT2018-77094, ASME Turbomachinery Technical Conference and Exposition, June 11-15, 2018, Oslo, Norway.
9. Choi, Y. S., Gottfried, D. A., and Fleeter, S., “Resonant Response of Mistuned Bladed Disks Including Aerodynamic Damping Effects,” *Journal of Propulsion and Power*, Vol. 25, No. 6, November–December 2009, pp. 1240-1248.
10. Hurty, W. C.: “Dynamic Analysis of Structural Systems Using Component Modes,” *AIAA Journal*, Vol. 3, No. 4, 1965, pp. 678–685.
11. Craig, R. R., Jr., Bampton, M. C. C., “Coupling of Substructures for Dynamics Analyses,” *AIAA Journal*, Vol. 6, No. 7, 1968, pp. 1313–1319.
12. Castanier, M. P., Óttarsson, G., Pierre, C., “A Reduced-Order Modeling Technique for Mistuned Bladed Disks,” *Journal of Vibration and Acoustics*, Vol. 119, No. 3, 1997, pp. 439–447.
13. R. Bladh, M. P. Castanier, C. Pierre, “Component-Mode-Based Reduced Order Modeling Techniques for Mistuned Bladed Disks—Part I: Theoretical Models,” *Journal of Engineering for Gas Turbines and Power*, January 2001, Vol. 123, pp. 89-99.
14. Baik, S., Castanier, M. P., Pierre, C., “Disk Design Methodology for Reducing Blade Vibration in Turbine Engine Rotors,” ASME Paper DETC2005-85741, Proceedings of the ASME 2005 International Design Engineering Technical Conferences & Computers and Information in Engineering Conference, September 2005.
15. Lim, S.-H., Bladh, R., Castanier, M. P., Pierre, C., “Compact, Generalized Component Mode Mistuning Representation for Modeling Bladed Disk Vibration,” *AIAA Journal*, Vol. 45, No. 9, September 2007.
16. He, Z., Epureanu, B. I., Pierre, C., “Fluid-Structural Coupling Effects on the Dynamics of Mistuned Bladed Disks,” *AIAA Journal*, Vol. 45, No. 3, March 2007.
17. Yang, M.-T., Griffin, J. H., “A Reduced Order Model of Mistuning Using a Subset of Nominal System Modes,” *Journal of Engineering for Gas Turbines and Power*, Vol. 123, No. 4, 2001, pp. 893–900.
18. Reddy, T.S.R., Min, J. B., Trudell, J. J., “Mistuned Bladed Disk Analysis with Unsteady Aerodynamics Using turbo-Reduce,” AIAA/ASME/ASCE/AHS/ASC Structures, Structural Dynamics & Materials, AIAA 2005-2028.
19. Kielb, R. E., Feiner, D. M., Griffin, J. H., and Miyakozawa, T., “Flutter of Mistuned Bladed Disks and Blisks with Aerodynamic and FMM Structural Coupling,” Proceedings of ASME Turbo Expo 2004, Vol. 6, ASME, New York, 2004, pp. 573–579.
20. K. J. Bathe, *Finite Element Procedures*. Prentice-Hall. Englewood Cliffs. 1996.
21. Whitehead, D. S., 1998, “The Maximum Factor by Which Forced Vibration of Blades Can Increase Due to Mistuning,” *Journal of Engineering for Gas Turbines and Power*, 120, 1998.
22. Bladh, R., Pierre, C., Castanier, M. P., and Kruse, M. J., “Dynamic Response Predictions for a Mistuned Industrial Turbomachinery Rotor Using Reduced-Order Modeling,” *Journal of Engineering for Gas Turbines and Power*, 124, 2002.
23. Kurstak, E., D’Souza, K. “Experimental Investigation of Mistuning and Damping Characteristics of a Bladed Disk at Operational Speed under Synchronous Vibration,” AIAA SciTech Forum, AIAA Paper 2020-1442, 2020.
24. Lim, S.-H., “Dynamic analysis and design strategies for mistuned bladed disks,” Ph.D. Thesis, University of Michigan, Ann Arbor, 2005.
25. D’Souza, K., private communication.